Int Ophthalmol (2019) 39:2245–2256
https://doi.org/10.1007/s10792-018-01060-x

ORIGINAL PAPER

Retinal vascular density evaluated by optical coherence tomography angiography in macular telangiectasia type 2

Berna Dogan · Muhammet Kazim Erol · Melih Akidan · Elcin Suren · Yusuf Akar

Received: 18 March 2018 / Accepted: 21 December 2018 / Published online: 3 January 2019

Abstract

Purpose To evaluate the retinal and choroidal vascular changes through optical coherence tomography angiography (OCTA) in patients with macular telangiectasia type 2 (MacTel 2).

Methods Our study included 20 patients (40 eyes) with MacTel 2, and age-matched and sex-matched 18 subjects (36 eyes) in the control group. Fundus color photographs, fundus autofluorescence, fundus fluorescein angiography, spectral-domain optical coherence tomography and OCTA were performed. Foveal vascular density and parafoveal vascular density (PFVD), and foveal retinal thickness and parafoveal retinal thickness, choroidal thickness (CT) and retinal ganglion cell–inner plexiform layer (GCIPL) were compared between MacTel 2 patients and normal age-matched controls.

Results The retinal whole vascular density and PFVD of the deep plexus were significantly lower in patients with MacTel 2 than that of the control group (56.93% vs. 58.54%, $p = 0.003$; and 60.38% vs. 61.66%, $p = 0.045$). The foveal avascular zone (FAZ) of the deep plexus was significantly enlarged in patients with MacTel 2 than that of the control group (0.44 vs. 0.36, $p = 0.009$). There was a positive and statistically significant correlation between the FAZ of the superficial and deep plexus and CT in patients with MacTel 2. There was a positive and statistically significant correlation between retinal whole, parafoveal temporal quadrant vascular density of the superficial and deep plexus and GCIPL thickness in patients with MacTel 2.

Conclusions Our study demonstrated that important retinal vascular density and FAZ changes in MacTel 2 occur in the deep capillary plexus of the retina.

Keywords Optical coherence tomography angiography · Macular telangiectasia type 2 · Vascular density · Retinal ganglion cell–inner plexiform layer · Choroidal thickness

B. Dogan (✉) · M. K. Erol · E. Suren
Department of Ophthalmology, Antalya Education and Research Hospital, Varlık Mah., Kazim Karabekir Caddesi, 07100 Antalya, Turkey
e-mail: bernadoga3@hotmail.com

M. K. Erol
e-mail: muhammetkazimerol@gmail.com

E. Suren
e-mail: elcin_baskan@yahoo.com

M. Akidan
Department of Ophthalmology, Kepez State Hospital, Antalya, Turkey
e-mail: melcihhh@yahoo.com

Y. Akar
Department of Ophthalmology, Akdeniz University Medical Faculty, Antalya, Turkey
e-mail: yakardr@hotmail.com

Introduction

Idiopathic macular telangiectasia type 2 (MacTel 2) is bilateral disease characterized by Müller cell dysfunction, changes in macular capillary network and neural atrophy [1]. Early manifestations of the disease include loss of retinal transparency, superficial retinal crystalline deposits, right-angled venules and presence of intraretinal cystoid spaces in the fovea. In later stages, the intraretinal pigment migrates, forming pigment plaques, and subretinal neovascular membrane (SNV) develops. There is not usually lipid exudation or hemorrhages associated with MacTel 2 unless SNV is present [2].

Fundus fluorescein angiography (FFA) has been considered for many years the gold standard for diagnosis of MacTel 2. The classic FFA finding is telangiectatic vessels that leak dye in the parafoveal area with fluorescein leakage not related to the cystic spaces [3]. Spectral-domain optical coherence tomography (SD-OCT) provides a useful visualization of the retinal and choroidal changes in patients with MacTel 2. SD-OCT has shown neurodegenerative changes in MacTel 2, including presence of hyporeflective spaces in the inner or outer retina, foveal thinning, intraretinal pigments, breaks in the ellipsoid zone with progressive outer retinal atrophy in which the retinal layers interior to the outer nuclear layer seemingly 'collapse' through these breaks toward the retinal pigment epithelium (RPE). Progression of the disease is characterized by shrinkage of the outer retinal layers and reduction in the central foveal thickness [4–6].

With the development of optical coherence tomography angiography (OCTA), it is now possible to noninvasively image the retinal and choroidal microvasculature without the use of exogenous intravenous dye injection. Both structural and blood flow information could be evaluated together via OCTA. Superficial and deep capillary plexus, vascular density and foveal avascular zone (FAZ) changes have been started to be evaluated through OCTA, and an effective imaging method has been obtained in the clarification of the pathophysiology of MacTel 2 [7, 8]. Since the response to anti-VEGF in the proliferative phase is good, OCTA seems to be more advantageous than other imaging methods regarding early detection of choroidal neovascularization (CNV) and planning the treatment.

In this study, we aimed to compare the superficial and deep retinal capillary density, choroidal vascular density, FAZ, choroidal thickness (CT) and ganglion cell–inner plexiform layer (GCIPL) in patient with MacTel 2 and control groups.

Materials and methods

Approval was obtained from the local ethics committee of University of Health Sciences, Antalya Training and Research Hospital, where the study was conducted and performed in compliance with the ethical standards set out in the Declaration of Helsinki. Before the participants were included in this study, their written informed consent was obtained.

All patients and controls underwent a comprehensive ophthalmologic examination, including measurements of best-corrected visual acuity (BCVA), slit lamp examination of the anterior segment, intraocular pressure, dilated fundus examination and OCTA imaging (Optovue RTVue XR 100 Avanti, Freemont, California, USA) and SD-OCT (Cirrus HD-OCT, Carl Zeiss Meditec, Dublin, CA, USA). Each patient with MacTel type 2 underwent color fundus photography, fundus autofluorescence (FAF) and FFA to confirm the diagnosis.

Inclusion criteria for the patient group were all eyes with either nonproliferative or proliferative MacTel type 2. The exclusion criteria for groups were as follows: Refractive error $> \pm 3$ spherical equivalent; poor image quality < 60 due to unstable fixation; intraocular pressure (IOP) > 21 mm Hg; preexisting macular pathologies, such as age-related macular degeneration, epiretinal membrane or macular hole; other retinopathies, such as retinal vascular occlusion, diabetic retinopathy or retinal dystrophy; preexisting ocular diseases, such as glaucoma, optic neuropathy or uveitis; previous vitreoretinal surgery or photodynamic therapy, diabetes mellitus, systemic arterial hypertension, cardiovascular diseases.

Spectral-domain optical coherence tomography

Spectral-domain OCT scans were obtained using the Cirrus HD-OCT. The Macular Cube 512×128 scan protocol was used for all subjects. The average, minimum (lowest GCIPL thickness over a single meridian crossing the annulus) and sectoral

(superotemporal, superior, superonasal, inferonasal, inferior, inferotemporal) GCIPL thicknesses were measured in an elliptical annulus around the fovea.

Optical coherence tomography angiography

The imaging of all subjects was performed with a commercial OCTA that had a scan rate of 70,000 A-scans/s, scan beam wavelength of 840 ± 10 nm and bandwidth of 45 nm. This device can do the volumetric scans of 304 × 304 A-scans at 70,000 A-scans/s in around 3.0 s [9]. All measurements were taken between 09:00 and 11:00 on the same day.

To evaluate the vascular structures, 3 × 3 mm OCT angiogram software was used. Split Spectrum Amplitude Decorrelation Angiography images were obtained. Images that could not be evaluated due to the low resolution were excluded. The OCTA images were independently graded and assessed by two clinicians. The software automatically segmented these full-thickness retinal scans into the superficial and deep inner retinal vascular plexuses, outer retina and choriocapillaris. The vascular density in superficial and deep retinal vascular zone was calculated automatically by this software, and FAZ was also automatically identified. The area 3 μm beneath the internal limiting membrane was defined as the starting line of the superficial capillary, which had sufficient thickness to contain the ganglion cell layer and the capillaries bounding the foveal avascular zone in the central macular region. The deep capillary plexus was imaged starting from 15 μm beneath the outer border of the inner plexiform layer and ending at 70 μm beneath the inner plexiform layer.

The same software also calculated the flow index rates in a central circular zone of 3.144 mm^2 in the outer retina and choriocapillaris segments.

Optical coherence tomography angiography was graded according to the lateral extension of vascular anomalies, using the foveal center as the main landmark: OCTA grade 1, vascular anomalies in the deep and/or superficial plexus temporal to the fovea; OCTA grade 2, vascular anomalies in the deep and/or superficial plexus temporal and nasal to the fovea; OCTA grade 3, markedly diffuse circumferentially vascular anomalies in the deep and superficial plexus; and OCTA grade 4, neovascularization in the outer retina with any OCTA signs of grade 1–3 [10].

Statistical analysis

Statistical analyses were performed using SPSS Statistics, version 22 (SPSS, Inc. Chicago, IL).To compare the groups, independent *t* test and Mann–Whitney *U* test were applied. The normality assumption for the independent variables was checked with Shapiro–Wilk test. The variables that were compliant with the normality assumption were subjected to the independent *t* test, while those that do not meet the normality assumption were subjected to Mann–Whitney *U* test. For the analysis of correlation, Pearson correlation coefficient and Spearman correlation coefficient were used. $p < 0.05$ was considered significant.

Results

Our study included 20 patients (40 eyes) with MacTel 2, and age-matched and sex-matched 18 subjects (36 eyes) in the control group. The mean age ± standard deviation (SD) was 56.2 ± 8.8 years in patients with MacTel 2 and 59.3 ± 10.2 years in the control group ($p = 0.328$).

Optical coherence tomography angiography provided detailed images of the retinal microcirculation in all patients with MacTel 2. In these patients, the most common findings on OCTA images were telangiectatic vessels, particularly evident in the deep plexus, intervascular spaces involving the superficial and the deep plexus in the foveal region, right-angled venules, FAZ irregularity and neovascularization.

The most common findings on OCT images were thinning and atrophy in the outer retina and inner segment/outer segment (IS/OS) layers, intraretinal hyporeflective cavitations, cystic formations in ganglion cell layer and inner nuclear layer, and internal limiting membrane (ILM) drape.

In MacTel 2 eyes, 24 of 40 eyes showed intraretinal hyporeflective cavitations; 8 eyes ILM drape; 31 eyes IS/OS bant defect; 9 eyes neovascularization. 9 (22.5%) of 40 eyes showed a grade-1 OCTA (Fig. 1); 18 eyes (45%) a grade 2 (Fig. 2); 4 eyes (10%) a grade 3 (Fig. 3); and 9 eyes (22.5%) a grade 4 (Fig. 4). No significant comparison was able to be performed between stages since there were not enough patients with different stages.

The classic FFA finding is telangiectatic vessels, dilated retinal capillaries and dilated blunted right-

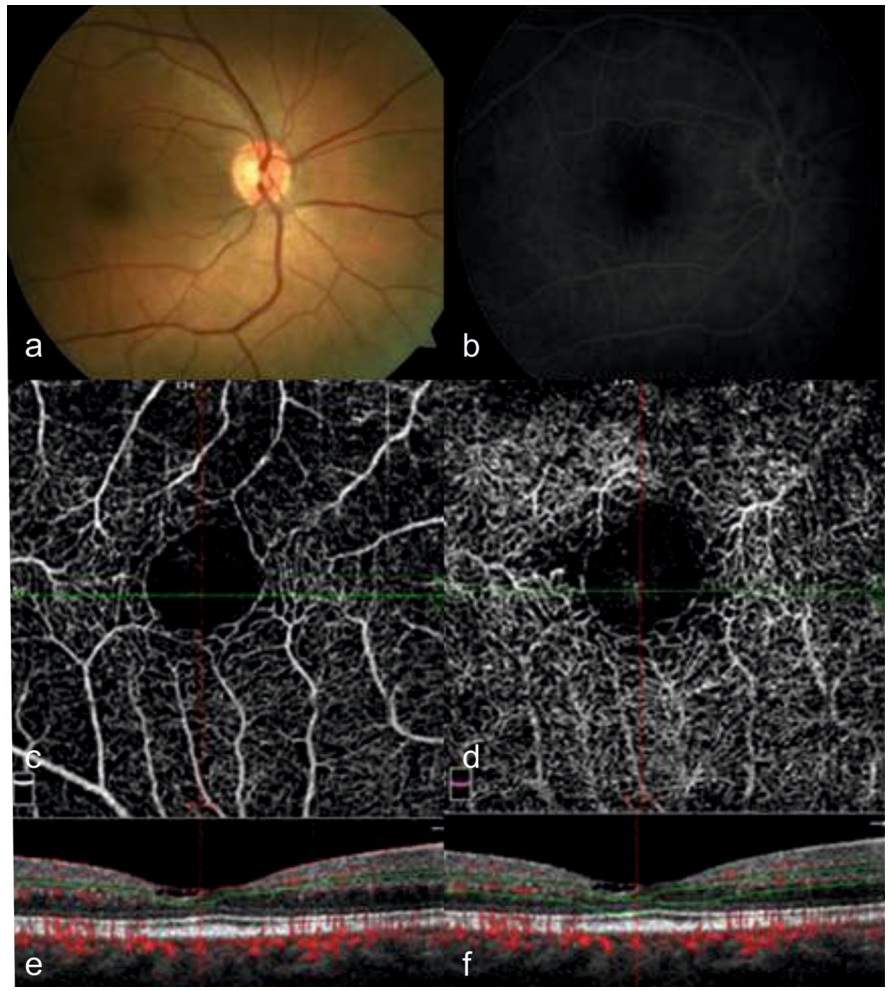

Fig. 1 Images from the right eye of a patient with the diagnosis of macular telangiectasia type 2. **a** Color fundus photography shows parafoveal loss of retinal transparency, **b** fundus fluorescein angiography, **c, d** optical coherence tomography angiography shows minimal increase in space between vessels in the superficial capillary plexus and increased space between vessels and mild telangiectatic changes in the deep capillary plexus temporal to the fovea (OCTA grade 1), **e**, **f** B-scan optical coherence tomography imaging shows intraretinal hyporeflective cavitation and internal limiting membrane drape

angled veins in patients with MacTel 2. Twenty-three eyes showed dilated retinal capillaries and telangiectatic vessels; 12 eyes dilated blunted right-angled veins.

The retinal whole vascular density of the superficial plexus was significantly lower in patients with MacTel 2 than that of the control group (50.89% vs. 52.58%, $p = 0.043$). Foveal vascular density and parafoveal vascular density (PFVD) of the superficial plexus were not significantly different between the two groups (26.83% vs. 26.63%, $p = 0.687$; and 53.54% vs. 54.64%, $p = 0.223$) There was a significant difference between choroidal flow rate ($p = 0.013$) and choroidal flow index ($p = 0.013$) in patients with MacTel 2 and control group. The mean CT was 328.9 ± 83.6 μm in patients with MacTel 2 and 290.6 ± 77.5 μm in control group ($p = 0.048$) (Table 1). The retinal whole vascular density and PFVD of the deep plexus were significantly lower in patients with MacTel 2 than that of the control group (56.93% vs. 58.54%, $p = 0.003$; and 60.38% vs. 61.66%, $p = 0.045$). The foveal vascular density of the deep plexus was not significantly different between the two groups (25.16% vs. 26.45%, $p = 0.346$). The foveal avascular zone of the deep plexus was significantly enlarged in patients with MacTel 2 than that of the control group (0.44 vs. 0.36, $p = 0.009$) (Table 2). There was a positive and statistically significant correlation between the FAZ of the superficial and deep plexus and CT in patients with MacTel 2. There was a negative and statistically significant correlation between the foveal vascular density, full-inner–outer retinal thickness and CT in patients with MacTel 2 (Table 3).

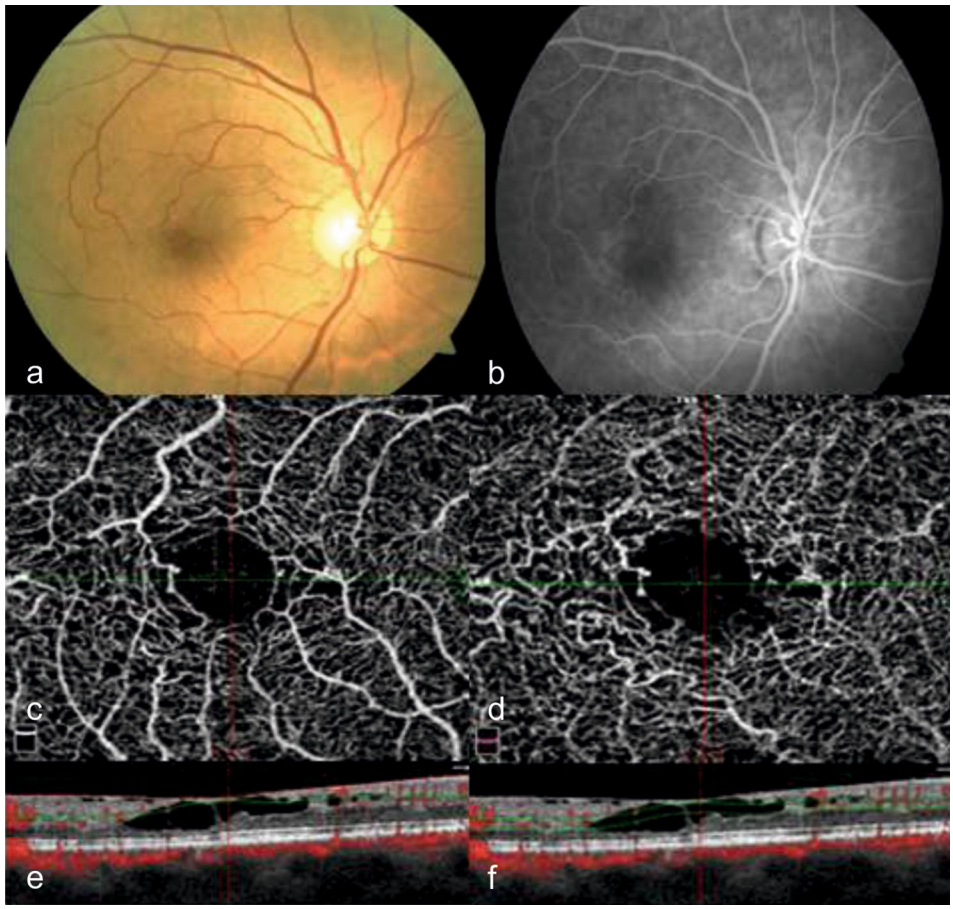

Fig. 2 Images from the right eye of a patient with the diagnosis of macular telangiectasia type 2. **a** Color fundus photography shows parafoveal loss of retinal transparency, **b** fundus fluorescein angiography reveals parafoveal hyperfluorescence, **c, d** optical coherence tomography angiography shows increase in space between vessels in the superficial capillary plexus and increased space between vessels and telangiectatic changes in the deep capillary plexus temporal and nasal to the fovea (OCTA grade 2), **e**, **f** B-scan optical coherence tomography imaging shows intraretinal hyporeflective cavitations, inner segment/outer segment bant defect and internal limiting membrane drape

Parafoveal retinal thickness in all quadrants was significantly different between the two groups (Table 4). Ganglion cell–inner plexiform layer in all quadrants was significantly lower in patients with MacTel 2 than that of the control group (Table 5). There was a positive and statistically significant correlation between retinal whole, parafoveal temporal quadrant vascular density of the superficial and deep plexus and GCIPL in patients with MacTel 2. There was a negative and statistically significant correlation between the FAZ of the superficial and deep plexus and GCIPL in patients with MacTel 2 (Table 6).

Discussion

MacTel 2 is an idiopathic neurodegenerative disease which causes a change in macular capillary network as well as vision loss. It is usually characterized by nonspecific symptoms until the proliferative stage [1, 3]. Although FFA is the gold standard imaging method for showing the dilated parafoveal capillary of the disease, it may be insufficient to show superficial and deep capillary plexus changes and accompanying subretinal neovascularization. OCTA has the typical advantages of OCT imaging, including the ability to detect abnormal microvascular structure in the parafoveal region, to diagnose MacTel 2, and to monitor its progression. OCTA is a noninvasive imaging method

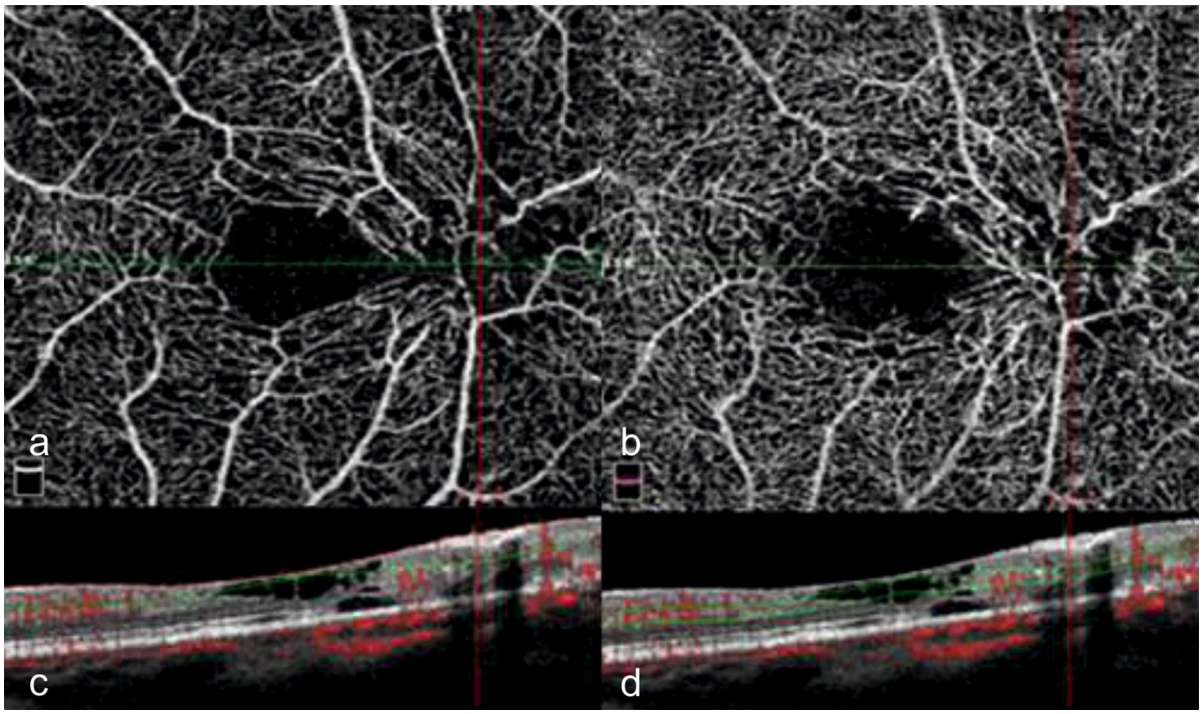

Fig. 3 Images from the left eye of a patient with the diagnosis of macular telangiectasia type 2. **a, b** Optical coherence tomography angiography shows markedly diffuse circumferential vascular anomalies with telangiectatic, distorted vessels in the superficial and deep capillary plexus (OCTA grade 3), **c, d** B-scan optical coherence tomography imaging shows marked intraretinal hyporeflective cavitation, inner segment/outer segment bant defect and internal limiting membrane drape

which helps to understand complex pathological changes [11]. This method shows the earliest changes in the temporal parafoveal deep capillary plexus, and these abnormalities extend circumferentially around the fovea up to the superficial capillary plexus and anastomotic choroidal extension. Additionally, data obtained from these scans provide quantitative measurements of the changes in retinal thickness [10, 12].

A study by Spaide et al. [13] showed changes in superficial and deep retinal plexus and patched loss-of-capillary vascular network in the advanced stages as well as telangiectatic vessels with increased intervascular spaces. Toto et al. [10] observed ectasia and more severe vascular anomalies, particularly in deep plexus.

In a study by Gass, telangiectatic vessels were suggested to change the structure of capillary walls, which prevents metabolic exchange [14]. The low-grade chronic nutritional injury may cause atrophy and degeneration of Müller cells and photoreceptor cells. Researchers later identified additional retinal abnormalities, and they emphasized the potential role of Müller cell abnormalities in MacTel 2 [15–17].

Müller cells are known to play important roles in the maintenance of foveal structural integrity, neuronal support and continuity of the blood–retina barrier [18, 19]. They provide many functions in the retina [20]. Müller cells manage liquid and electrolyte concentrations in the retina [21], mediate several effects caused by cytokines and growth factors [22] and produce a wide variety of growth factors including proangiogenic and antiangiogenic factors [23, 24]. Müller cells provide nutritional and regulatory support to both retinal neurons and vascular cells. Müller cell ablation causes both neuronal and vascular pathologies including photoreceptor apoptosis, vascular telangiectasis and eventual intraretinal neovascularization [25]. Müller cell is an important manager of vascular endothelial growth factor in the retina and loss, or defective function of Müller cells may alter growth patterns of intraretinal neovascularization [24, 26].

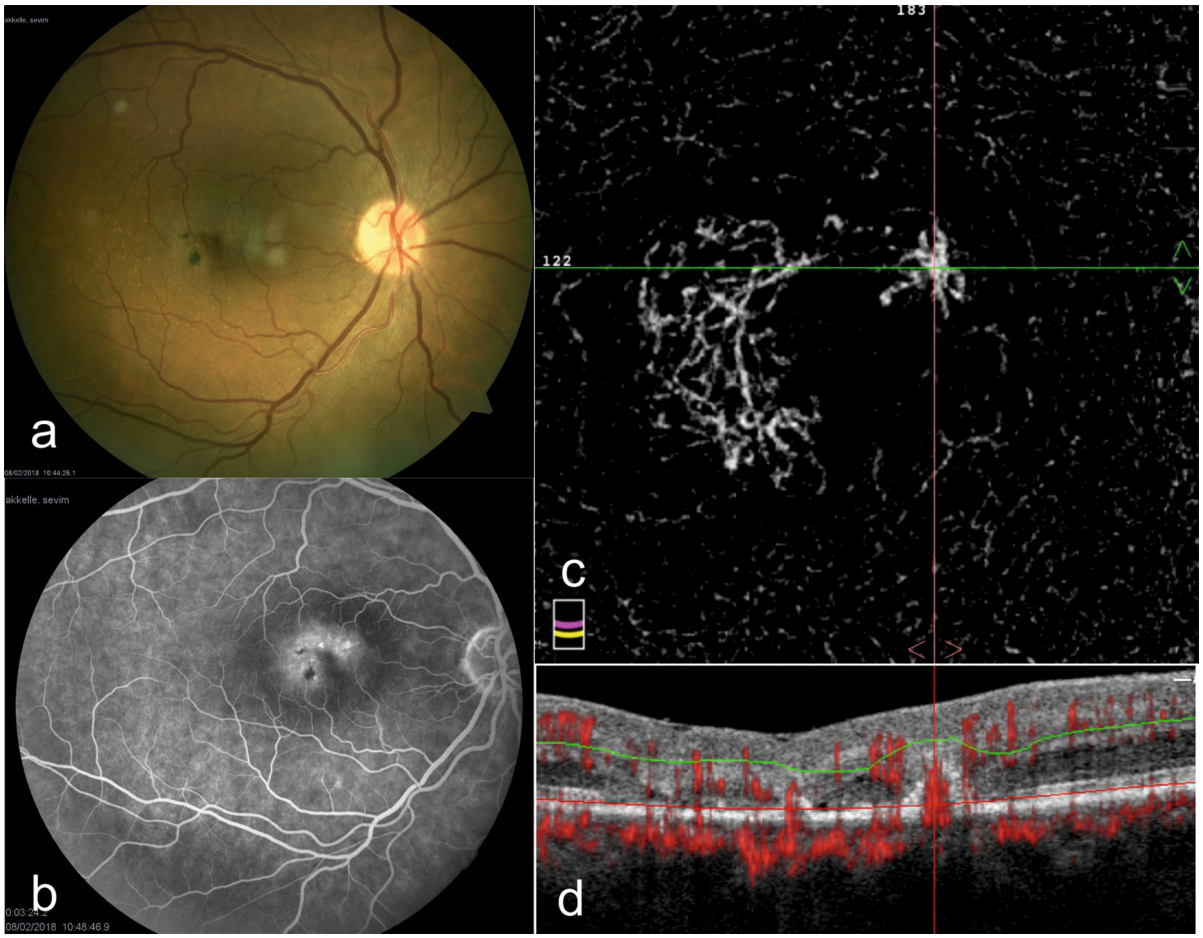

Fig. 4 Images from the right eye of a patient with the diagnosis of macular telangiectasia type 2. **a** Color fundus photography shows foveal pigment clumps with perilesional loss of retinal transparency, **b** fundus fluorescein angiography reveals subfoveal hyperfluorescence, **c** optical coherence tomography angiography shows markedly neovascular proliferation in the outer retina (OCTA grade 4), **d** B-scan optical coherence tomography imaging reveals neovascularization

As opposed to the first vascular theory proposed by Gass et al. [27], degeneration of Müller cells, which support protective and supportive functions, is currently thought as a primary pathology, and retinal layer damage, atrophy and vascular changes are thought to be emerged secondarily [3].

Based on the presence of dilated retinal arterioles and subretinal blood, Gass and Oyakawa [2] have suggested that neovascularization associated with MacTel 2 may develop anastomosis through choroidal circulation. OCTA imaging shows the relationship between subretinal neovascular complexes and choroidal circulation [9]. In previous studies, subretinal neovascularization was considered to be due to primarily from the retinal circulation. However, nowadays, the neovascular complex has been found to communicate frequently with both retinal and choroidal circulation [11]. In a study by Engelbrecht et al. [28], eyes with MacTel 2 were evaluated, and chorioretinal anastomosis was reported to occur always before the subretinal neovascularization.

Whether MacTel 2 patients have increased choroidal thickness is controversial. While Chhablani et al. [29] did not observe any significant difference in the choroidal thickness of 41 MacTel 2 patients from India as compared to sex- and age-matched controls, Nunes et al. [30] found the mean choroidal thickness to be 41 µm greater in a cohort of 62 MacTel 2 patients in the USA than a group of sex- and age-matched controls. Nunes et al. [30] suggested that a thick

Table 1 Foveal and parafoveal vascular density of the superficial plexus, and choroidal flow rate evaluated by OCTA in patients with MacTel 2 and control group

	Patients with MacTel 2 (n = 40 eyes of 20 subjects)	Control group (n = 36 eyes of 18 subjects)	p value[a]
Vascular density of the superficial plexus (%)			
Whole	50.89 ± 3.02	52.58 ± 2.56	**0.043**
Fovea	26.83 ± 4.18	26.63 ± 4.93	0.687
Parafovea	53.54 ± 3.69	54.64 ± 3.38	0.223
Superior hemisphere	51.98 ± 8.51	54.60 ± 3.35	0.189
Inferior hemisphere	53.83 ± 3.44	54.69 ± 3.60	0.199
Temporal	52.83 ± 3.92	53.71 ± 3.26	0.327
Superior	53.75 ± 5.28	55.79 ± 3.63	0.181
Nasal	52.98 ± 4.72	54.03 ± 3.62	0.372
Inferior	54.44 ± 3.38	55.09 ± 4.21	0.199
Foveal avascular zone (mm^2)	0.41 ± 0.16	0.34 ± 0.08	0.089
Choroidal flow rate	1.90 ± 0.06	1.93 ± 0.05	**0.013**
Choroidal flow index	0.614 ± 0.06	0.610 ± 0.04	**0.013**
Choroidal thickness (μm)	328.9 ± 83.6	290.6 ± 77.5	**0.048**

Bold value represents statistical significance

OCTA optical coherence tomography angiography

[a]Mann–Whitney *U* test

Table 2 Foveal and parafoveal vascular density of the deep plexus evaluated by OCTA in patients with MacTel 2 and control group

	Patients with MacTel 2 (n = 40 eyes of 20 subjects)	Control group (n = 36 eyes of 18 subjects)	p value
Vascular density of the deep plexus (%)			
Whole	56.93 ± 2.27	58.54 ± 2.22	**0.003**[a]
Fovea	25.16 ± 6.18	26.45 ± 4.88	0.346[a]
Parafovea	60.38 ± 2.7	61.66 ± 2.52	**0.045**[a]
Superior hemisphere	60 ± 3.36	61.31 ± 2.77	0.169[b]
Inferior hemisphere	60.75 ± 2.69	61.71 ± 2.66	0.132[a]
Temporal	58.90 ± 3.32	60.84 ± 2.60	**0.009**[a]
Superior	60.98 ± 4.46	62.74 ± 2.94	0.222[b]
Nasal	59.28 ± 4.32	60.79 ± 2.95	0.157[b]
Inferior	61.83 ± 2.78	62.46 ± 3.02	0.365[a]
Foveal avascular zone (mm^2)	0.44 ± 0.13	0.36 ± 0.09	**0.009**[a]

Bold value represents statistical significance

OCTA optical coherence tomography angiography

[a]Independent *t* test

[b]Mann–Whitney *U* test

choroid may be an early manifestation of MacTel 2 eyes and may be useful for diagnosis. While the role of the choroid in MacTel 2 is unknown, it is plausible that Müller cell dysfunction may lead to compensatory choroidal changes. Another explanation may be that the choroidal thickness may increase in response to an increase in the outward production of the vascular endothelial growth factor by RPE. Kumar et al. [31] reported the co-occurrence of MacTel 2 with pachychoroid group of disorders. It is possible that a subset of these patients of MacTel with thick choroid go on to develop clinical manifestations of pachychoroid disorders.

In our study, the choroid was found to be significantly thicker in patients with MacTel 2 than in control group. There was a positive and statistically significant correlation between the foveal avascular zone of the superficial and deep plexus and choroidal thickness in patients with MacTel 2. Therefore, we believe that the increase in choroidal thickness in the patient group has been developed as a compensator against the disease. A thickened choroid may be an

Table 3 Correlation between choroidal thickness and OCTA parameters

	r	*p* value
Vascular density of the superficial plexus (%)		
Whole	− 0.008	0.949[a]
Fovea	− 0.242	**0.037**[a]
Parafovea	0.083	0.479[a]
Foveal avascular zone (mm^2)	0.322	**0.005**[a]
Vascular density of the deep plexus (%)		
Whole	0.074	0.534[b]
Fovea	− 0.234	0.054[b]
Parafovea	0.212	0.076[b]
Foveal avascular zone (mm^2)	0.331	**0.005**[b]
Choroidal flow rate	0.036	0.761[a]
Choroidal flow index	0.034	0.771[a]
Full thickness	− 0.510	**0.00**[a]
Inner thickness	− 0.528	**0.00**[a]
Outer thickness	− 0.336	**0.003**[a]

Bold value represents statistical significance

OCTA optical coherence tomography angiography

[a]Spearman's correlation coefficient test

[b]Pearson correlation coefficient test

early manifestation of MacTel 2, and it may be a valuable diagnostic clue to identify these patients.

In addition, our study demonstrated that the retinal whole vascular density and parafovea and temporal quadrant vascular density of the deep plexus were significantly lower in patients with MacTel 2 than that of the control group. The temporal parafoveal deep capillary plexus is the first area affected with progressive capillary rarefaction and dilation and abnormal capillary anastomosis. Secondary changes extend to the entire fovea and the superficial plexus, with abnormal dilated anastomoses between both the plexuses [32]. Muller cells are involved in the control of angiogenesis and the regulation of retinal blood flow. The lesions of Muller cells eventually result in extensive abnormal changes in retinal blood vessels, such as the loss of capillary density [33]. Muller cells degeneration may play an important role in capillary vascular density.

In the present study, the parafoveal retinal thickness and GCIPL thickness decreased in all quadrants in patients with MacTel 2. There was a positive and statistically significant correlation between retinal whole, temporal quadrant vascular density of the superficial and deep plexus and GCIPL in patients with MacTel 2. Our study demonstrated that in eyes with MacTel 2, there was significant RGCs degeneration. These findings are suggestive of neurodegeneration in MacTel 2. Ganglion cells degeneration may play an important role of MacTel 2 pathogenesis as well as Muller cells.

Neurons, glia (Muller cells and astrocytes) and blood vessels interact during all aspects of metabolic function to form a functional energy unit. The ordered

Table 4 Parafoveal thickness evaluated by OCTA in patients with MacTel 2 and control group

	Patients with MacTel 2 (n = 40 eyes of 20 subjects)	Control group (n = 36 eyes of 18 subjects)	*p* value[a]
Full thickness	228.53 ± 42.01	248.5 ± 26.49	**0.004**
Parafovea-nasal	293.45 ± 27.71	317.72 ± 21.39	**0.00**
Parafovea-superior	293 ± 33.59	317.39 ± 21.35	**0.00**
Parafovea-temporal	278.55 ± 27.41	303.89 ± 22.74	**0.00**
Parafovea-inferior	289.08 ± 22.04	314.36 ± 19.09	**0.00**
Inner thickness	65.18 ± 18.51	68.5 ± 14.38	0.225
Parafovea-nasal	109.9 ± 14.29	128.31 ± 12.66	**0.00**
Parafovea-superior	116.7 ± 18.05	130.33 ± 13.18	**0.00**
Parafovea-temporal	109 ± 14.80	120.19 ± 14.80	**0.001**
Parafovea-inferior	110.93 ± 13.44	128.97 ± 11.16	**0.00**
Outer thickness	163.3 ± 28.77	179.89 ± 15.47	**0.00**
Parafovea-nasal	183.5 ± 17.51	190.31 ± 18.93	0.151
Parafovea-superior	176.23 ± 24.84	187.08 ± 15.13	**0.001**
Parafovea-temporal	169.65 ± 14	180.97 ± 21.28	**0.00**
Parafovea-inferior	175.63 ± 21.1	185.89 ± 11.97	**0.011**

Bold value represents statistical significance

OCTA optical coherence tomography angiography

[a]Mann–Whitney *U* test

Table 5 Ganglion cell–inner plexiform layer evaluated by SD-OCT in patients with MacTel 2 and control group

	Patients with MacTel 2 (n = 40 eyes of 20 subjects)	Control group (n = 36 eyes of 18 subjects)	p value[a]
GCIPL location (μm)			
Average	71.18 ± 13.08	83.44 ± 4.2	**0.00**
Minimum	65.11 ± 15.07	78.31 ± 6.2	**0.001**
Superior	73 ± 13.5	84.81 ± 6.5	**0.00**
Inferior	72.04 ± 13.07	79.94 ± 4.9	**0.004**
Superotemporal	72.07 ± 13.13	82.62 ± 7.4	**0.002**
Inferotemporal	73.21 ± 13.13	83.06 ± 3.7	**0.001**
Superonasal	71.43 ± 14.89	84.19 ± 5.6	**0.00**
Inferonasal	70.89 ± 15.46	83.44 ± 4.5	**0.00**

Bold value represents statistical significance

GCIPL ganglion cell–inner plexiform layer, *SD-OCT* spectral-domain optical coherence tomography

[a]Mann–Whitney U test

functioning of the metabolic unit may arguably be critical for the RGCs; impaired functioning secondary to Muller cells loss may lead to structural alterations and degeneration of the neurosensory retina, including RGCs [34]. Additionally, after photoreceptor degeneration, there is a progressive retinal degeneration that affects all retinal layers, displacement of the inner retinal vessels that cross the nerve fiber layer, dragging the RGC axons. Finally, due to vessel traction of their axons, there is an impairment of the axonal transport and the RGCs die [35]. It is not known exactly which mechanisms of degenerative events have begun, but it can be considered that the mechanisms act jointly and increase the effectiveness of each other.

The classic FFA finding is telangiectatic vessels, dilated retinal capillaries and dilated blunted right-angled veins in patients with MacTel 2. Garcia et al. [36] demonstrated that statistical analysis did not indicate significant difference between area measurements obtained with FFA and OCTA in patients diagnosed with diabetic macular ischemia. There is very limited literature on natural history of MacTel 2 coexistent with diabetes mellitus. Additional systemic associations (e.g., hypertension) are likely to contribute to the progression of MacTel 2 [37].

Our study has some limitations. One of the most important limitations is that this study was conducted with a small cohort of patients. No significant comparison was able to be performed between stages since there were not enough patients with different stages. To our knowledge, this is the first study that evaluated the correlation between retinal vascular density, FAZ changes, CT and GCIPL.

In conclusion, OCTA provides valuable information regarding disease severity, disease progression and follow-up, and neovascularization activity in patients with MacTel 2. Our study demonstrated that the earliest changes were shown to be observed in deep

Table 6 Correlation between GCIPL and OCTA parameters

	r	p value[a]
Vascular density of the deep plexus (%)		
Whole	0.404	**0.007**
Fovea	0.19	0.228
Parafovea	0.298	0.053
Superior hemisphere	0.252	0.103
Inferior hemisphere	0.343	**0.024**
Temporal	0.495	**0.001**
Superior	0.074	0.638
Nasal	0.157	0.326
Inferior	0.207	0.182
Foveal avascular zone (mm^2)	− 0.304	**0.048**
Vascular density of the superficial plexus (%)		
Whole	0.370	**0.015**
Fovea	− 0.05	0.748
Parafovea	0.241	0.12
Superior hemisphere	0.273	0.077
Inferior hemisphere	0.238	0.125
Temporal	0.314	**0.04**
Superior	0.138	0.379
Nasal	0.094	0.555
Inferior	0.19	0.221
Foveal avascular zone (mm^2)	− 0.356	**0.019**
Choroidal flow rate	0.334	**0.029**
Choroidal flow index	0.336	**0.028**

Bold value represents statistical significance

GCIPL ganglion cell–inner plexiform layer, *OCTA* optical coherence tomography angiography

[a]Spearman's correlation coefficient test

capillary plexus, parafovea and temporal quadrant vascular density, foveal avascular zone of the deep capillary plexus, GCIPL and choroid. Further studies are needed to validate the prognostic value of these findings.

Compliance with ethical standards

Conflict of interest All authors declare that they have no conflict of interest.

Ethical approval All procedures performed in studies involving human participants were in accordance with the ethical standards of the institutional and/or national research committee and with the 1964 Declaration of Helsinki and its later amendments or comparable ethical standards.

Informed consent Informed consent was obtained from all individual participants included in the study.

References

1. Yannuzzi LA, Bardal AM, Freund KB, Chen KJ, Eandi CM, Blodi B (2006) Idiopathic macular telangiectasia. Arch Ophthalmol 124(4):450–460
2. Gass JD, Oyakawa RT (1982) Idiopathic juxtafoveolar retinal telangiectasis. Arch Ophthalmol 100(5):769–780
3. Wu L, Evans T, Arevalo JF (2013) Idiopathic macular telangiectasia type 2 (idiopathic juxtafoveolar retinal telangiectasis type 2A, Mac Tel 2). Surv Ophthalmol 58(6):536–559
4. Maruko I, Iida T, Sekiryu T, Fujiwara T (2008) Early morphological changes and functional abnormalities in group 2A idiopathic juxtafoveolar retinal telangiectasis using spectral domain optical coherence tomography and microperimetry. Br J Ophthalmol 92(11):1488–1491
5. Albini TA, Benz MS, Coffee RE, Westfall AC, Lakhanpal RR, McPherson AR, Holz ER (2006) Optical coherence tomography of idiopathic juxtafoveolar telangiectasia. Ophthalmic Surg Lasers Imaging 37(2):120–128
6. Paunescu LA, Ko TH, Duker JS, Chan A, Drexler W, Schuman JS, Fujimoto JG (2006) Idiopathic juxtafoveal retinal telangiectasis: new findings by ultrahigh-resolution optical coherence tomography. Ophthalmology 113(1):48–57
7. Thorell MR, Zhang Q, Huang Y, An L, Durbin MK, Laron M, Sharma U, Stetson PF, Gregori G, Wang RK, Rosenfeld PJ (2014) Swept-source OCT angiography of macular telangiectasia type 2. Ophthalmic Surg Lasers Imaging Retina 45(5):369–380
8. Chidambara L, Gadde SG, Yadav NK, Jayadev C, Bhanushali D, Appaji AM, Akkali M, Khurana A, Shetty R (2016) Characteristics and quantification of vascular changes in macular telangiectasia type 2 on optical coherence tomography angiography. Br J Ophthalmol 100(11):1482–1488
9. de Carlo TE, Romano A, Waheed NK, Duker JS (2015) A review of optical coherence tomography angiography (OCTA). Int J Retina Vitreous 1:5
10. Toto L, Di Antonio L, Mastropasqua R, Mattei PA, Carpineto P, Borrelli E, Rispoli M, Lumbroso B, Mastropasqua L (2016) Multimodal imaging of macular telangiectasia type 2: focus on vascular changes using optical coherence tomography angiography. Invest Ophthalmol Vis Sci 57(9):OCT268–OCT276
11. Zhang Q, Wang RK, Chen CL, Legarreta AD, Durbin MK, An L, Sharma U, Stetson PF, Legarreta JE, Roisman L, Gregori G, Rosenfeld PJ (2015) Swept source OCT angiography of neovascular macular telangiectasia type 2. Retina 35(11):2285–2299
12. Roisman L, Rosenfeld PJ (2016) Optical coherence tomography angiography of macular telangiectasia type 2. Dev Ophthalmol 56:146–158
13. Spaide RF, Klancnik JM, Cooney MJ (2015) Retinal vascular layers in macular telangiectasia type 2 imaged by optical coherence tomographic angiography. JAMA Ophthalmol 133(1):66–73
14. Gass JDM (1997) Stereoscopic atlas of macular diseases: diagnosis and treatment, vol 1, 4th edn. Mosby, St Louis
15. Koizumi H, Slakter JS, Spaide RF (2007) Full-thickness macular hole formation in idiopathic parafoveal telangiectasis. Retina 27(4):473–476
16. Cohen SM, Cohen ML, El-Jabali F, Pautler SE (2007) Optical coherence tomography findings in nonproliferative group 2a idiopathic juxtafoveal retinal telangiectasis. Retina 27(1):59–66
17. Powner MB, Gillies MC, Zhu M, Vevis K, Hunyor AP, Fruttiger M (2013) Loss of Muller's cells and photoreceptors in macular telangiectasia type 2. Ophthalmology 120(11):2344–2352
18. Bringmann A, Iandiev I, Pannicke T, Wurm A, Hollborn M, Wiedemann P, Osborne NN, Reichenbach A (2009) Cellular signaling and factors involved in Müller cell gliosis: neuroprotective and detrimental effects. Prog Retin Eye Res 28(6):423–451
19. Unterlauft JD, Eichler W, Kuhne K, Yang XM, Yafai Y, Wiedemann P, Reichenbach A, Claudepierre T (2012) Pigment epithelium-derived factor released by Müller glial cells exerts neuroprotective effects on retinal ganglion cells. Neurochem Res 37(7):1524–1533
20. Fletcher EL, Downie LE, Ly A, Ward MM, Batcha AH, Puthussery T, Yee P, Hatzopoulos KM (2008) A review of the role of glial cells in understanding retinal disease. Clin Exp Optom 91(1):67–77
21. Newman EA (1993) Inward-rectifying potassium channels in retinal glial (Müller) cells. J Neurosci 13(8):3333–3345
22. Wahlin KJ, Campochiaro PA, Zack DJ, Adler R (2000) Neurotrophic factors cause activation of intracellular signaling pathways in Müller cells and other cells of the inner retina, but not photoreceptors. Invest Ophthalmol Vis Sci 41(3):927–936
23. Behzadian MA, Wang XL, Al-Shabrawey M, Caldwell RB (1998) Effects of hypoxia on glial cell expression of angiogenesis-regulating factors VEGF and TGF-beta. Glia 24(2):216–225

24. Bai Y, Ma JX, Guo J, Wang J, Zhu M, Chen Y, Le YZ (2009) Müller cell-derived VEGF is a significant contributor to retinal neovascularization. J Pathol 219(4):446–454
25. Shen W, Fruttiger M, Zhu L, Chung SH, Barnett NL, Kirk JK, Lee S, Coorey NJ, Killingsworth M, Sherman LS, Gillies MC (2012) Conditional Müller cell ablation causes independent neuronal and vascular pathologies in a novel transgenic model. J Neurosci 32(45):15715–15727
26. Rodrigues M, Xin X, Jee K, Babapoor-Farrokhran S, Kashiwabuchi F, Ma T, Bhutto I, Hassan SJ, Daoud Y, Baranano D, Solomon S, Lutty G, Semenza GL, Montaner S, Sodhi A (2013) VEGF secreted by hypoxic Müller cells induces MMP-2 expression and activity in endothelial cells to promote retinal neovascularization in proliferative diabetic retinopathy. Diabetes 62(11):3863–3873
27. Gass JD, Blodi BA (1993) Idiopathic juxtafoveolar retinal telangiectasis: update of classification and follow-up study. Ophthalmology 100(10):1536–1546
28. Engelbrecht NE, Aaberg TM Jr, Sung J, Lewis ML (2002) Neovascular membranes associated with idiopathic juxtafoveolar telangiectasis. Arch Ophthalmol 120(3): 320–324
29. Chhablani J, Kozak I, Jonnadula GB, Venkata A, Narayanan R, Pappuru RR, Rao PS (2014) Choroidal thickness in macular telangiectasia type 2. Retina 34(9):1819–1823
30. Nunes RP, Goldhardt R, de Amorim CA, Thorell MR, Abbey AM, Kuriyan AE, Modi YS, Shah M, Yehoshua Z, Gregori G, Feuer W, Rosenfeld PJ (2015) Spectral-domain optical coherence tomography measurements of choroidal thickness and outer retinal disruption in macular telangiectasia type 2. Ophthalmic Surg Lasers Imaging Retina 46(2):162–170
31. Kumar V, Kumar P, Ravani R, Gupta P (2018) Macular telangiectasia type II with pachychoroid spectrum of macular disorders. Eur J Ophthalmol 1:1120672118769527. https://doi.org/10.1177/1120672118769527
32. Spaide RF, Suzuki M, Yannuzzi LA, Matet A, Behar-Cohen F (2017) Volume-rendered angiographic and structural optical coherence tomography angiography of macular telangiectasia type 2. Retina 37(3):424–435
33. Mao L, Weng SS, Gong YY, Yu SQ (2017) Optical coherence tomography angiography of macular telangiectasia type 1: comparison with mild diabetic macular edema. Lasers Surg Med 49(3):225–232
34. Yu DY, Cringle SJ, Balaratnasingam C, Morgan WH, Yu PK, Su EN (2013) Retinal ganglion cells: energetics, compartmentation, axonal transport, cytoskeletons and vulnerability. Prog Retin Eye Res 36:217–246
35. García-Ayuso D, Salinas-Navarro M, Agudo-Barriuso M, Alarcón-Martínez L, Vidal-Sanz M, Villegas-Pérez MP (2011) Retinal ganglion cell axonal compression by retinal vessels in light-induced retinal degeneration. Mol Vis 17:1716–1733
36. Garcia JM, Lima TT, Louzada RN, Rassi AT, Isaac DL, Avila M (2016) Diabetic macular ischemia diagnosis: comparison between optical coherence tomography angiography and fluorescein angiography. J Ophthalmol 2016:3989310
37. Jhingan M, Marsonia K, Shukla D, Rosenfeld PJ, Chhablani J (2017) Idiopathic macular telangiectasis type 2 and coexistent diabetic retinopathy. Int J Retina Vitreous 25(3):50